Article:
Xiao, C., Van Vliet, S., Bliem, R. et al. (2023) Electrochemically-stimulated nanoscale mechanochemical wear of silicon. Friction, 11 (11). pp. 2142-2152. ISSN: 2223-7690

https://doi.org/10.1007/s40544-023-0764-4

Friction **11**(11): 2142–2152 (2023)
https://doi.org/10.1007/s40544-023-0764-4
ISSN 2223-7690
CN 10-1237/TH
RESEARCH ARTICLE

Electrochemically-stimulated nanoscale mechanochemical wear of silicon

Chen XIAO[1,2], Stefan VAN VLIET[1], Roland BLIEM[1,2], Bart WEBER[1,2], Steve FRANKLIN[1,3,*]

[1] *Advanced Research Center for Nanolithography (ARCNL), Amsterdam 1098XG, the Netherlands*

[2] *Van der Waals–Zeeman Institute, Institute of Physics, University of Amsterdam (UvA), Amsterdam 1098XG, the Netherlands*

[3] *Department of Materials Science and Engineering, The University of Sheffield, Sheffield S13JD, UK*

Received: 24 December 2022 / Revised: 15 February 2023 / Accepted: 21 March 2023

Abstract: Mechanochemical reactions at the sliding interface between a single-crystalline silicon (Si) wafer and a silica (SiO_2) microsphere were studied in three environmental conditions: humid air, potassium chloride (KCl) solution, and KCl solution with an applied voltage. Compared to that from humid air, mechanochemical material removal from the silicon surface increased substantially in the KCl-immersed condition, and further increased when electrochemistry was introduced into the tribological system. By measuring the load dependence of the material removal rate and analyzing the results using a mechanically assisted Arrhenius-type kinetic model, the activation energy (E_a) and the mechanical energy (E_m), by which this energy is reduced by mechanical activation, were compared qualitatively under different environmental conditions. In the KCl-immersed condition, mechanochemistry may decrease the required effective energy of reactions ($E_{eff} = E_a - E_m$) and promote material removal mainly through improved catalysis of the mechanochemical reactions facilitated by greater availability of water molecules compared to the humid air condition. Thus, the effectiveness of the mechanochemistry is improved. In the electrochemical condition, electrochemically-accelerated oxidation of the silicon surface was confirmed by the X-ray photoelectron spectroscopy (XPS) characterization. The results strongly suggest that electrochemistry further stimulates mechanochemical reactions primarily by increasing the initial energy state of the surface via the facilitated formation of interfacial bonding bridges, i.e., a surface oxidation/hydroxylation process.

Keywords: spherical contact; adhesive wear; normal loading; power law

1 Introduction

Mechanochemical reactions, also called tribochemical reactions if they occur at tribological interfaces involving relative motion, are prevalent at solid material interfaces across length scales, resulting in the transfer of material atoms due to the breakage of chemical bonds [1–6]. Such reactions play a role in many applications ranging from the processing of material surfaces to the undesired wear of the moving and contacting parts of nano-/micro-electromechanical systems (NEMS/MEMS) [7, 8]. Electrochemistry influences the mechanochemical reactions considerably. For example, electrochemically-assisted material processing can be very effective in improving the efficiency of material removal from surfaces [9–11]. However, mechanically-influenced electrochemical corrosion can greatly reduce the lifetime of devices such as marine equipment (e.g., valves, bearings, shafts, and hydraulic system) used in a corrosive environment and NEMS/MEMS operating in humid environments [8, 12–17]. Although the previous studies have empirically investigated the contribution of electrochemistry to mechanochemical reactions, the interplay

*Corresponding author: Steve FRANKLIN, E-mail: s.franklin@arcnl.nl

between electrochemistry and mechanical activation in mechanochemical reactions is still largely unclear owing to the complexity of the coupling between mechanical, chemical, and electrochemical effects.

In Refs. [18–20], by performing nanowear tests based on the atomic force microscopy (AFM) and nanoindentation, interfacial mechanochemical reactions in single asperity contacts were investigated for precisely controlled the load/contact pressure (P), contact time, velocity (v), and sliding trajectory. In this way, attempts were made to reveal the mechanochemical removal mechanisms that take place at elastically deformed contacts. The mechanochemical reactions occurring at the interface of the silicon (Si) surface and the silica (SiO_2) microsphere could be described as having three stages: (i) surface hydroxylation by water molecules, (ii) formation of "Si–O–Si" bonding bridges across the interface by dehydration reactions of the hydroxyl (OH) groups at the interface, and (iii) atomic attrition via the rupture of the Si–Si bond of the silicon substrate with mechanical activation [20–24].

With the view to predicting and regulating the mechanochemical reactions at tribological interfaces, the variation of the mechanochemical removal with the contact pressure is well described by the mechanically assisted Arrhenius-type kinetic model [20, 25, 26]. Mechanochemical reactions could occur through lowering the activation energy (E_a), which is the difference between the energies of the initial state and the activated state, to a new value of the effective energy (E_{eff}) [27, 28]. The degree, to which this energy difference is reduced, can be ascribed to the mechanical energy (E_m) channeled along the reaction coordinate. Then, E_{eff} can be expressed by Eq. (1) [25, 29–31]:

$$E_{eff} = E_a - E_m \tag{1}$$

The mechanochemical reaction rate constant or normalized yield (k) can then be modeled with a modified Arrhenius-type equation [29, 31–35].

$$k = A\exp\frac{-(E_a - E_m)}{k_B T} \tag{2}$$

where A is the pre-exponential factor (the units of which depend on the units of the left-hand side of the equation), T is the average temperature of the sliding interface, and k_B (= 1.38×10^{-23} J/K) is the Boltzmann constant. The E_m term can be further described as the shear stress of the sliding contact (σ) multiplied by a volume term. The latter is often called the critical activation volume (ΔV^*) and considered to be associated with the physical deformation of the reacting species due to applied shear [25, 29–31]. The previous literature shows that the E_{eff} of the mechanochemical reaction coordinate changes via the variation of E_a and E_m (or ΔV^*), depending on surface chemistry [20, 36], surface structure [37], counter surface [38], environmental media [20], etc. Based on the above research basis, electrochemistry, as a newly introduced energy input into mechanochemical systems, has the potential to provide new insights into mechanochemical reaction theory and novel ideas for practical applications of surface machining and wear protection.

In this work, the mechanochemical reaction rates of a Si/SiO_2 interface are determined by the material removal volume and compared under the same loading conditions in humid air and immersed in potassium chloride (KCl) solution without and with an applied voltage. Based on the load dependence of the mechanochemical removal results, the contributions of mechanochemistry and electrochemistry in the mechanochemical reactions at the tribological interfaces are analyzed using the mechanically assisted Arrhenius-type kinetic model (Eq. (2)). The facilitating effect of mechanochemical reactions by surface oxidation during the electrochemical corrosion process, confirmed by the X-ray photoelectron spectroscopy (XPS) characterization, is discussed.

2 Experimental

2.1 Materials

Boron-doped silicon wafers (University Wafer, USA) with the (100) orientation and 500 μm in thickness were used for mechanochemical wear tests using the AFM (Dimension Icon, Bruker, USA) equipped with an electrochemical cell, as shown in Fig. 1(a). Before the nanowear tests, the native oxide layer on the silicon wafer was removed by immersion in 5 wt% hydrofluoric acid (HF) solution for 3 min. The samples were then ultrasonically cleaned with ethanol and deionized water in sequence, and dried using pure

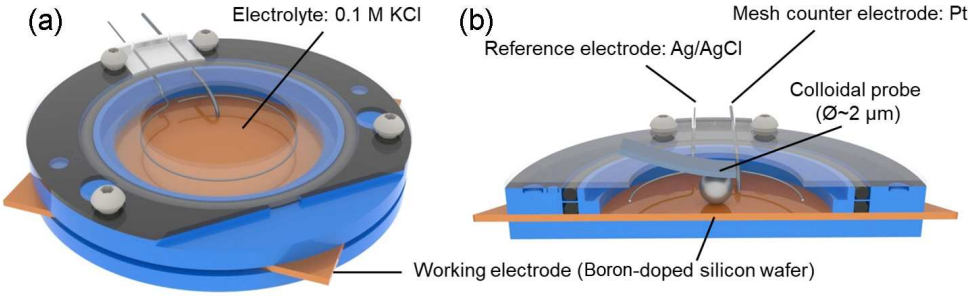

Fig. 1 Schematic of electrochemical-atomic force microscopy (EC-AFM) setup: (a) isometric view of EC-AFM cell and (b) cutaway view of EC-AFM setup equipped with colloidal silica probe. Note: Φ is the diameter of the colloidal probe. Reproduced with permission from Ref. [39], © The Authors 2022.

N_2 gas. The root-mean-square surface roughness of the HF treated silicon surface was measured to be less than 0.5 nm over a square scanned area of 5 μm × 5 μm using a sharp Si AFM tip (RTESPA-300, Bruker, USA) with a nominal diameter of approximately 20 nm.

2.2 Nanowear tests and XPS characterization

All the electrochemical, nanowear, and topographical experiments were performed using an AFM equipped with an electrochemical cell module, as shown in Fig. 1. For the nanowear tests, a silica microsphere with a diameter of approximately 2 μm, attached to a cantilever with a spring constant of approximately 42 N/m, was rubbed in a linear reciprocating manner on the Si wafer. For a total normal load (F_n) range of 1.25–10 μN, which is the sum of the applied F_n and the adhesion force (pull-off force, Fig. S1 in the Electronic Supplementary Material (ESM)), the maximum P was calculated to be 0.95–1.75 GPa based on Derjaguin–Muller–Toporov (DMT) contact mechanics [40]. The number of reciprocating sliding cycles (N) was 200, the stroke length (L) was 4 μm, and the v was 8 μm/s. The material removal behavior of the hydrophobic silicon wafer surface by the silica microsphere was compared for three different environments: humid air with a relative humidity (RH) of ~50%, 0.1 M KCl (Sigma Aldrich, USA) solution, and 0.1 M KCl solution with an applied voltage of 0.5 V. These three environments are denoted as MC(g), MC(l), and MC+EC. At least 3 repeated experiments were performed for each set of experimental conditions; the same silica microsphere was used for different load conditions under the same environment. In order to estimate the surface topography changes to the colloid microspheres after the nanowear tests, different microspheres were used for different environmental conditions, and the apexes of the colloid microsphere before and after the nanowear test were characterized by scanning on a calibration grating sample (TGT1, TipsNano, EST). During the nanowear test in electrochemical conditions (MC+EC), the Si sample was mounted in contact with two gold-plated spring pins that provided the electrical connection with the working electrode (WE). A circular area of 35 mm in diameter on the silicon surface was exposed to electrolyte solution of 0.1 M KCl, and Pt and Ag|AgCl wires served as the counter and reference electrodes (CE and RE), respectively. All potentials were given with reference to the RE (Ag|AgCl) using an electrochemical workstation with a bipotentiostat (CHI760E, CH Instruments, USA).

To determine the influence of electrochemical corrosion on the chemical composition and atomic structure of the silicon surface, the XPS (HiPP-3 Analyzer (entrance slit: 1.0 mm), Scienta Omicron, Germany) using a monochromatic Al Kα source was performed on the silicon surface after electrochemical corrosion for 30 min in 0.1 M KCl solution with an applied voltage of 0.5 V. For reference, the XPS spectra were also made for silicon surfaces that were freshly HF-etched and that had been immersed in KCl for 30 min without an applied voltage.

3 Results and discussion

3.1 Mechanochemical material removal processes in humid air and KCl solution with and without voltage

The nanowear tests (silica microsphere sliding against silicon surface) were performed in humid air and

KCl solution with and without voltage as a function of the applied F_n, as illustrated in Figs. 2(a), 2(d), and 2(g). After the wear tests, the wear tracks were scanned using a sharp silicon AFM tip with a radius of 10 nm. The topographic images (Figs. 2(b), 2(e), and 2(h)) and the average cross-sectional profiles (Figs. 2(c), 2(f), and 2(i)) of the wear scars on the silicon surfaces are shown in Fig. 2. The applied contact pressures, ranging from 0.95 to 1.7 GPa, were chosen to be much lower than the yield stress of Si (11.3–13 GPa). Therefore, material removal can be assumed to be dominated by interfacial mechanochemical reactions at the Si/SiO_2 interface rather than mechanical interactions, and the material removal rate can be considered to be the rate of those reactions [19]. Regarding the wear in the electrochemical condition (Figs. 2(g)–2(i)), the shape of the nanowear tracks are very similar to those observed for the other environmental conditions, which may suggest that the wear was entirely caused by mechanochemical reaction, and that pure electrochemical corrosion without mechanical activation did not play a significant role in the material removal.

Figure 3 plots the mechanochemical k as a function of F_n and P, which is estimated by the removal volume normalized with the total sliding time. The removal volume was calculated by the integral calculation of the average cross-sectional area (Figs. 2(c), 2(f), and 2(i)) over the whole L. When F_n and P increased from 1.25 μN and 0.95 GPa to 10 μN and 1.75 GPa, respectively, the removal rate increased from 0.1×10^4 to 3.5×10^4 nm^3/s in humid air, from 0.6×10^4 to 4.2×10^4 nm^3/s in KCl-immersed condition, and from 1.1×10^4 to 5.0×10^4 nm^3/s in the electrochemical condition. These results indicate that electrochemistry strongly influences the mechanochemical reactions taking place at the sliding interface of Si/SiO_2. Figure S2 in the ESM shows that the friction force occurring during the nanowear process in humid air is slightly higher than that in KCl-immersed solution with and without voltage. This trend, which is opposite to that of the wear results, indicates that changes in the friction behavior are not responsible for the observed significant enhancement of the material removal behavior. Reference [20] has shown that OH groups originating from water molecules or free radicals are involved in the key steps of interfacial mechanochemical reactions. Comparing the humid air environment to

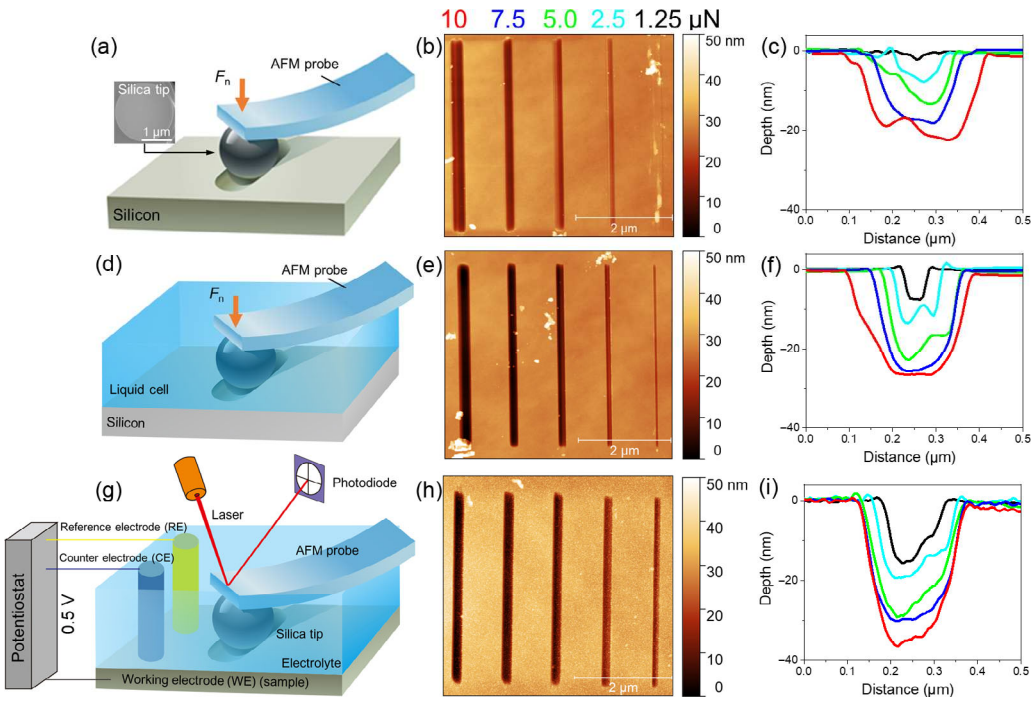

Fig. 2 (a, d, g) Schematic illustration of mechanochemical wear test of silicon surface with silica sphere attached to AFM system, (b, e, h) AFM images of nanowear scars, and (c, f, i) average cross-sectional profiles: (a–c) in humid air, (d–f) in KCl solution without voltage, and (g–i) in KCl solution with voltage.

the KCl-immersed condition (without voltage), we assume that with the latter, the involvement of more water molecules within the contact area promotes the mechanochemical reactions at the interface, and thus the material removal from the silicon surface to a greater degree. When electrochemistry is introduced into the tribological system, the mechanochemical reactions are further facilitated by electrochemical corrosion. It is important to note that there is a critical load, below which no material removal takes place. In humid air, the critical load (the x intercept of the trend in Fig. 3(a)) is estimated to be about 1.0 μN, and it decreases to nearly zero in KCl solution and electrochemical conditions due to the more intensive mechanochemical reactions.

Figure S3 in the ESM displays the AFM images and cross-sectional profiles of the silica microsphere before and after the reciprocating wear tests in the three environmental conditions. The protrusion observed on the silica microsphere (which is hydrophilic) after the nanowear test in humid air can be attributed to capillary adhesion [41–43], which readily attracts wear debris to the apex of the sphere. Since capillary adhesion can be neglected when immersed in liquid, and because the Si–O bond energy (452 kJ/mol) of the silica microsphere is much higher than that of the Si–Si back bond (228 kJ/mol) on the silicon substrate [44], no wear or wear debris was observed on the silica microsphere after the nanowear experiments conducted in KCl solution without voltage. However, in the KCl electrochemical condition, some electrochemical wear took place on the silica microsphere. To mitigate this small effect, each of the three individual data sets used to obtain the average values and error bars in Fig. 3 is obtained by testing three times over the full range of F_n (1.25–10 μN).

3.2 Mechanical activation effect in electro-mechanochemical material removal processes

To investigate the interplay between electrochemistry and mechanical activation, the results of the load dependence of the material removal (Fig. 3) are analyzed using the modified Arrhenius-type kinetics model (Eq. (2)). The k is obtained from the removal/reaction rate in Fig. 3, assuming that the silicon material is removed atom-by-atom, and that the atomic scale wear is governed by mechanochemical reactions. The E_m term in Eq. (2) can be written as the product of σ and the ΔV^* change under mechanical shear action: $E_m = \sigma\Delta V^*$. Here, dividing Amontons' law of friction by the contact area, σ can be estimated to change linearly with P, with the friction coefficient (μ) as a proportionality constant: $\sigma = \sigma_0 + \mu P$, where σ_0 is a non-zero pressure-independent residual term [34, 45, 46]. More details regarding the derivation can be found in Section S1 in the ESM. Inserting this expression to Eq. (2) and taking the logarithm of both sides give Eq. (3) [31, 36].

$$\ln k = \ln A - \frac{E_a}{k_B T} + \frac{\sigma_0 V^*}{k_B T} + \frac{V^* P}{k_B T} \tag{3}$$

Figure 4(a) shows the semi-log plots of k as a function of P, including linear fits to the data, from which a slope and offset can be extracted (Fig. 4(b)). The material removal data point for a low contact pressure of 0.95 GPa obtained in humid air is much

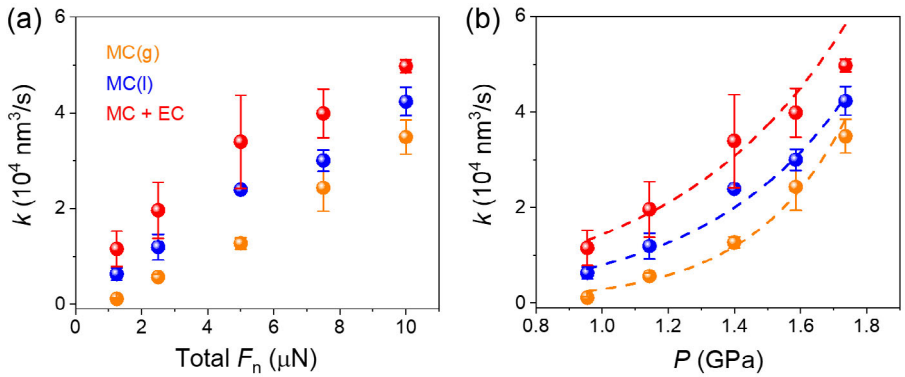

Fig. 3 k as a function of (a) total F_n and (b) P. The removal volume is obtained by the integration of the average cross-sectional area over the L (as in Figs. 2(c), 2(f), and 2(i)).

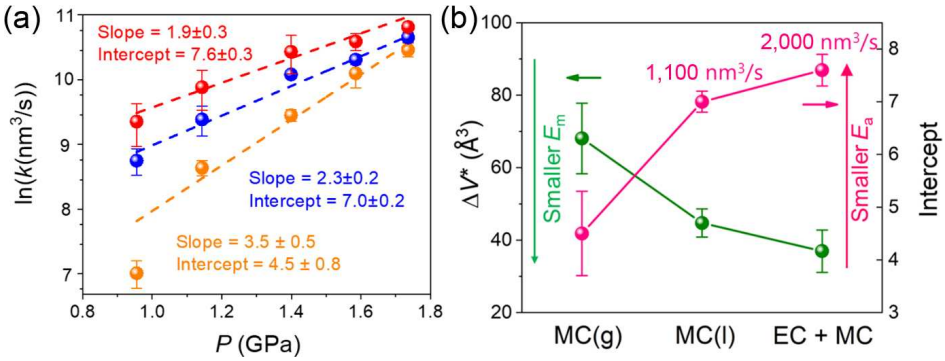

Fig. 4 (a) Semi-log plots of P dependence of k for wear tracks formed on silicon samples in humid air (orange) and KCl solution without (blue) and with (red) voltage. 200 sliding cycles were imposed at a sliding v of 8 μm/s. (b) ΔV^* (mechanical activation, green) and intercept (activation energy, pink) in three environmental conditions in (a).

lower than the estimated value. This may be attributed to the poor contact condition at a low contact pressure at the reaction interface (as determined by the real contact area), combined with the limited availability of reactant (water) in comparison to the two conditions (with and without an applied voltage), where the sample is fully immersed in solution [47]. The situation is improved when sufficient water molecules available as reactants or higher contact pressures, are involved in the mechanochemical reactions. The slopes indicate the ΔV^*, which is considered in Refs. [26, 31] to be associated with mechanical activation when an external mechanical force is applied. A higher slope value implies a larger E_m during the mechanochemical reactions. Since the measured friction force and coefficient did not vary greatly for the three environmental conditions (Fig. S2 in the ESM), the slopes in Fig. 4 can be used to give a qualitative comparison between the ΔV^* values for these conditions. The intercept qualitatively reflects the magnitude of E_a for the reaction pathway in the absence of mechanical interaction when the contact pressure is above the threshold value to initiate the mechanochemical reactions, and an increase in the intercept value indicates a decrease in E_a. An absolute value of E_a cannot be calculated from the intercept value because the A term is not accurately known; however, it is assumed to be constant for the three environmental conditions [36], so the intercept values can be used for qualitative comparison of the effects of the environmental conditions on E_a.

Comparing the results from the humid air and KCl solution environments, the material removal rate was increased in the latter by enhanced mechanochemistry. We observed that the estimated slope in the relation between the removal rate and contact pressure decreases significantly, but the intercept increases, which implies that both E_a and E_m decrease (Fig. 4(b)). These results indicate that the interfacial mechanochemical reactions have a higher self-driven force or tendency, and that less mechanical activation is needed in the KCl-immersed condition. According to the material removal/mechanochemical reaction rate measured by nanowear tests, E_{eff} (MC(g)) > E_{eff} (MC(l)). It can be hypothesized that the decrease in E_a is greater than the decrease in E_m according to Eq. (1) when the mechanochemistry is facilitated by the increased water availability at the tribological interface, where water molecules effectively act as the chemical catalyst, most likely in steps i and ii (Fig. 5(a)) [22]. When electrochemistry was introduced into the tribological interface, the reaction rate was further increased by electrochemically-stimulated mechanochemical reactions, in this case showing a similar slope value (which is an indication of E_m) but an intercept value indicating a twofold increase in wear (reaction) rate, and thus a much larger decrease in E_a (Fig. 4(b)). This indicates that electrochemistry decreases the E_{eff} without greatly changing the mechanical activation effect (E_m). Therefore, this decrease in E_a for the electro-mechanochemical condition compared to that of the mechanochemical condition seems not directly attributable to mechanical activation but mainly due to a different effect.

To further elucidate how electrochemistry influences the mechanochemical removal of silicon, the chemical

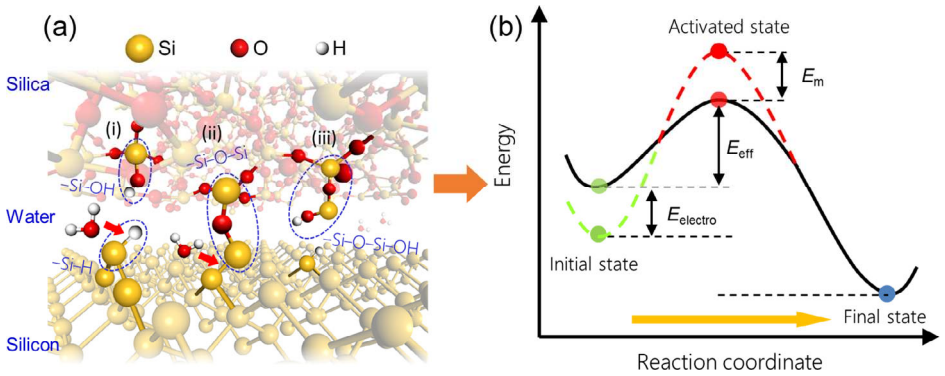

Fig. 5 (a) Illustration showing the mechanochemical removal process. Reproduced with permission from Ref. [20], © American Chemical Society 2019. (b) Schematic energy diagram along hypothetical reaction coordinate leading to the mechanochemical removal of silicon by SiO_2 microsphere in humid air and KCl solution without and with voltage. Note: $E_{electro}$ is the contribution of electrochemistry to the more chemically active initial state.

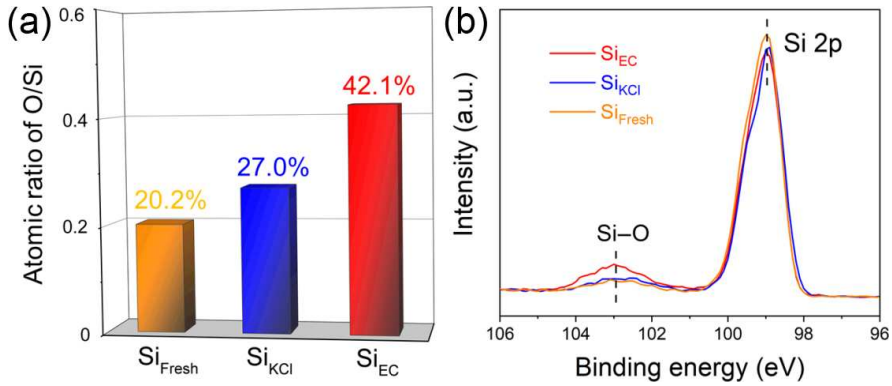

Fig. 6 (a) Comparison of atomic ratios relative to Si 2p determined by the XPS of Si_{fresh}, Si_{KCl}, and Si_{EC}. (b) Si 2p narrow XPS spectra of Si_{fresh}, Si_{KCl}, and Si_{EC}.

compositions of the silicon substrate before and after electrochemical corrosion were characterized by the XPS. Fig. S4 in the ESM illustrates how the XPS samples were prepared, in each case using freshly HF-etched silicon surfaces (Si_{fresh}) as the starting condition, which was measured as a reference. The XPS measurements were carried out on samples subjected to electrochemical corrosion in 0.1 M KCl solution with an applied voltage of 0.5 V for 30 min (Si_{EC}). This was compared to Si_{fresh} after immersion in 0.1 KCl solution without voltage for 30 min (Si_{KCl}), so that the contribution of static etching by water molecules to the surface oxidation could be distinguished from the electrochemical effect. Table S1 in the ESM displays the elemental compositions of Si_{fresh}, Si_{KCl}, and Si_{EC} measured by the XPS. The presence of oxygen on the Si_{fresh} may be attributed to residual oxides on the surface adsorbed from the environment, and is a good benchmark for estimating the surface oxidation of the Si_{KCl} and Si_{EC}. Upon corrosion, a slight oxygen increase can be observed on the Si_{KCl}, but a much larger increase can be observed on the Si_{EC} (Fig. 6(a)). The high-resolution Si 2p XPS spectra of Si_{fresh}, Si_{KCl}, and Si_{EC} (Fig. 6(b)) show that the oxidized silicon (Si–O) peak at 102.9 eV grows at the expense of the elemental Si peak at 99.2 eV [48]. Thus, it is shown that surface oxidation during electrochemical corrosion is much more pronounced than corrosion as a result of immersion in KCl solution without an applied voltage. The XPS results suggest that the Si_{EC} surface has the largest oxygen concentration, and therefore this supports the estimation made by the fitted intercept values (Fig. 4(a)): The Si_{EC} surface has the highest reaction tendency (the lowest E_a) for interfacial mechanochemical reactions.

Based on Refs. [15–19], the mechanochemical reactions at the interface of Si/SiO_2 can be described by a model involving the formation of "Si–O–Si"

bonding bridges across the sliding interface and the rupture of the Si–Si network with the assistance of a mechanical shear action (Fig. 5(a)). The formation rate of the "Si–O–Si" bonding bridges is governed by the number of terminated OH groups on the silicon substrate, which are formed by the oxidation/hydroxylation reactions of the H-terminated Si_{fresh} surface with water molecules in the environment [49]. Compared with static chemical etching without an applied voltage, oxidation reactions can be accelerated during the electrochemical corrosion process [50, 51], as supported by the work presented here. This promotes an initial stable equilibrium state with a higher chemical activity/energy level and makes it easier for the reaction barrier to be overcome, as shown in the simplified chemical reaction coordinate in Fig. 5(b). Future studies into the details of this process may be conducted for instance through atomistic computer simulations. To differentiate the role of mechanochemistry, the contribution of electrochemistry to the more chemically active initial state is denoted as "$E_{electro}$", giving a smaller E_{eff} (= $E_a - E_m - E_{electro}$). Based on the hypothesis above, mechanochemistry decreases the required energy of reactions and promotes material removal mainly by mechanical activation, and electrochemistry stimulates reactions by favoring the chemistry activity/energy state of the initial surface via a surface oxidation/hydroxylation process.

4 Summary and conclusions

In this work, mechanochemical reactions occurring at a sliding interface between a silicon wafer and a silica microsphere were measured and compared in humid air (50% RH), KCl solution, and KCl solution with an applied voltage. Using a mechanically assisted Arrhenius-type kinetic model and elastic contact mechanics, insights into the mechanical activation for mechanochemical reactions at the Si/SiO_2 interfaces were obtained from the measured load dependence of the material removal rate. Comparing humid air and KCl solution conditions (without an applied voltage), material removal from the silicon surface was found to increase substantially. This enhanced mechanochemical reaction may be mainly attributable to a reduction in the E_a required for mechanochemical reaction as a result of improved catalysis facilitated by the greater availability of water molecules. When electrochemistry is introduced into the tribological system, the material removal rate is further increased by electrochemical stimulation of the mechanochemical reactions. In the electrochemical condition, the results indicate that the mechanical activation for mechanochemical reactions does not change greatly, but that the E_a decreases substantially, which may be attributable to an increase in the chemical activity or energy state of the initial surface. It is hypothesized that electrochemically-accelerated oxidation of the silicon surface, confirmed by the XPS characterization, contributes to the electro-mechanochemical reactions via the facilitated formation of interfacial bonding bridges. The findings of this study provide deeper insights into the mechanistic understanding of electrochemically-stimulated mechanochemical reactions that can play an important role in many practical applications such as chemical–mechanical polishing and wear protection in NEMS/MEMS.

Acknowledgements

This work has been carried out at Advanced Research Center for Nanolithography (ARCNL), a public-private partnership of University of Amsterdam (UvA), Vrije University Amsterdam (VU), the Dutch Research Council (NWO), and the semiconductor equipment manufacturer (Advanced Semiconductor Material Lithography (ASML)). Bart WEBER acknowledges funding from the NWO VENI (Grant No. VI.Veni.192.177).

Declaration of competing interest

The authors have no competing interests to declare that are relevant to the content of this article.

Author contributions

Chen XIAO: conceptualization, methodology, validation, formal analysis, data curation, and writing—original draft. **Stefan VAN VLIET:** methodology, formal analysis, data curation, and writing—review & editing.

Roland BLIEM: resources, formal analysis, and writing—review & editing. **Bart WEBER:** resources, formal analysis, writing—review & editing, and funding acquisition. **Steve FRANKLIN:** conceptualization, supervision, formal analysis, writing—review & editing, and funding acquisition.

Electronic Supplementary Material: Supplementary material is available in the online version of this article at https://doi.org/10.1007/ s40544-023-0764-4.

References

[1] Xue Y R, Li X, Li H B, Zhang W K. Quantifying thiol–gold interactions towards the efficient strength control. *Nat Commun* **5**: 4348 (2014)

[2] Zhai W Z, Bai L C, Zhou R H, Fan X L, Kang G Z, Liu Y, Zhou K. Recent progress on wear-resistant materials: Designs, properties, and applications. *Adv Sci* **8**(11): 2003739 (2021)

[3] James S L, Friščić T. Mechanochemistry. *Chem Soc Rev* **42**(18): 7494–7496 (2013)

[4] Martini A, Eder S J, Dörr N. Tribochemistry: A review of reactive molecular dynamics simulations. *Lubricants* **8**(4): 44 (2020)

[5] Guo J, Gao J, Xiao C, Chen L, Qian L M. Mechanochemical reactions of GaN–Al_2O_3 interface at the nanoasperity contact: Roles of crystallographic polarity and ambient humidity. *Friction* **10**(7): 1005–1018 (2022)

[6] Leriche C, Franklin S, Weber B. Measuring multi-asperity wear with nanoscale precision. *Wear* **498–499**: 204284 (2022)

[7] Xiao C, Hsia F C, Sutton-Cook A, Weber B, Franklin S. Polishing of polycrystalline diamond using synergies between chemical and mechanical inputs: A review of mechanisms and processes. *Carbon* **196**: 29–48 (2022)

[8] Kim S H, Asay D B, Dugger M T. Nanotribology and MEMS. *Nano Today* **2**(5): 22–29 (2007)

[9] Zhang L F, Lu D, Deng H. Study on material removal mechanisms in electrochemical etching-enhanced polishing of GaN. *J Manuf Process* **73**: 903–913 (2022)

[10] Chen Z J, Zhao Y H. Investigation into electrochemical oxidation behavior of 4H-SiC with varying anodizing conditions. *Electrochem Commun* **109**: 106608 (2019)

[11] Zhai W J. Research progress in tribo-electrochemistry and tribo-electrochemical polishing. *Front Mech Eng-PRC* **2**(4): 463–467 (2007)

[12] Lingwall B A, Sexton T N, Cooley C H. Polycrystalline diamond bearing testing for marine hydrokinetic application. *Wear* **302**(1–2): 1514–1519 (2013)

[13] Conlisk A T. *Essentials of Micro- and Nanofluidics: With Applications to the Biological and Chemical Sciences*. Cambridge (UK): Cambridge University Press, 2012.

[14] Berradja A. Metallic glasses for triboelectrochemistry systems. In: *Metallic Glasses—Properties and Processing*. Huang H, Ed. London (UK): IntechOpen, 2018: 77–109.

[15] Zhou F, Ma Q, Wang Q Z, Zhou Z F, Li L K Y. Electrochemical and tribological properties of CrBCN coatings with various B concentrations in artificial seawater. *Tribol Int* **116**: 19–25 (2017)

[16] Fu Y Q, Zhou F, Zhang M D, Wang Q Z, Zhou Z F. Structure and tribocorrosion behavior of CrMoSiCN nanocomposite coating with low C content in artificial seawater. *Friction* **9**(6): 1599–1615 (2021)

[17] Zhang X G, Zhang Y L, Jin Z M. A review of the bio-tribology of medical devices. *Friction* **10**(1): 4–30 (2022)

[18] Xiao C, Deng C B, Zhang P, Qian L M, Kim S H. Interplay between solution chemistry and mechanical activation in friction-induced material removal of silicon surface in aqueous solution. *Tribol Int* **148**: 106319 (2020)

[19] Xiao C, Chen C, Guo J, Zhang P, Chen L, Qian L M. Threshold contact pressure for the material removal on monocrystalline silicon by SiO_2 microsphere. *Wear* **376–377**(A): 188–193 (2017)

[20] Xiao C, Xin X J, He X, Wang H B, Chen L, Kim S H, Qian L M. Surface structure dependence of mechanochemical

etching: Scanning probe-based nanolithography study on Si(100), Si(110), and Si(111). *ACS Appl Mater Interfaces* **11**(23): 20583–20588 (2019)

[21] Wen J L, Ma T B, Zhang W W, Psofogiannakis G, van Duin A C T, Chen L, Qian L M, Hu Y Z, Lu X C. Atomic insight into tribochemical wear mechanism of silicon at the Si/SiO_2 interface in aqueous environment: Molecular dynamics simulations using ReaxFF reactive force field. *Appl Surf Sci* **390**: 216–223 (2016)

[22] Yeon J, van Duin A C T, Kim S H. Effects of water on tribochemical wear of silicon oxide interface: Molecular dynamics (MD) study with reactive force field (ReaxFF). *Langmuir* **32**(4): 1018–1026 (2016)

[23] Chen L, Wen J L, Zhang P, Yu B J, Chen C, Ma T B, Lu X C, Kim S H, Qian L M. Nanomanufacturing of silicon surface with a single atomic layer precision via mechanochemical reactions. *Nat Commun* **9**: 1542 (2018)

[24] Luo C S, Jiang Y L, Liu Y Q, Wang Y, Sun J H, Qian L M, Chen L. Role of interfacial bonding in tribochemical wear. *Front Chem* **10**: 852371 (2022)

[25] Jacobs T D B, Carpick R W. Nanoscale wear as a stress-assisted chemical reaction. *Nat Nanotechnol* **8**(2): 108–112 (2013)

[26] Martini A, Kim S H. Activation volume in shear-driven chemical reactions. *Tribol Lett* **69**(4): 150 (2021)

[27] Fernández-Bertran J F. Mechanochemistry: An overview. *Pure Appl Chem* **71**(4): 581–586 (1999)

[28] Beyer M K, Clausen-Schaumann H. Mechanochemistry: The mechanical activation of covalent bonds. *Chem Rev* **105**(8): 2921–2948 (2005)

[29] Gosvami N N, Bares J A, Mangolini F, Konicek A R, Yablon D G, Carpick R W. Mechanisms of antiwear tribofilm growth revealed *in situ* by single-asperity sliding contacts. *Science* **348**(6230): 102–106 (2015)

[30] Chen L, Xiao C, He X, Yu B J, Kim S H, Qian L M. Friction and tribochemical wear behaviors of native oxide layer on silicon at nanoscale. *Tribol Lett* **65**(4): 139 (2017)

[31] Yeon J, He X, Martini A, Kim S H. Mechanochemistry at solid surfaces: Polymerization of adsorbed molecules by mechanical shear at tribological interfaces. *ACS Appl Mater Interfaces* **9**(3): 3142–3148 (2017)

[32] Beyer M K. The mechanical strength of a covalent bond calculated by density functional theory. *J Chem Phys* **112**(17): 7307–7312 (2000)

[33] Gotsmann B, Lantz M A. Atomistic wear in a single asperity sliding contact. *Phys Rev Lett* **101**(12): 125501 (2008)

[34] Spikes H. Stress-augmented thermal activation: Tribology feels the force. *Friction* **6**(1): 1–31 (2018)

[35] Tysoe W. On stress-induced tribochemical reaction rates. *Tribol Lett* **65**(2): 48 (2017)

[36] He X, Kim S H. Surface chemistry dependence of mechanochemical reaction of adsorbed molecules—An experimental study on tribopolymerization of α-pinene on metal, metal oxide, and carbon surfaces. *Langmuir* **34**(7): 2432–2440 (2018)

[37] Xiao C, Li J, Guo J, Zhang P, Yu B J, Chen L, Qian L M. Role of mechanically-driven distorted microstructure in mechanochemical removal of silicon. *Appl Surf Sci* **520**: 146337 (2020)

[38] Xiao C, Chen C, Wang H B, Chen L, Jiang L, Yu B J, Qian L M. Effect of counter-surface chemistry on defect-free material removal of monocrystalline silicon. *Wear* **426–427**(B): 1233–1239 (2019)

[39] Xiao C, Elam F, van Vliet S, Bliem R, Lépinay S, Shahidzadeh N, Weber B, Franklin S. Intercrystallite boundaries dominate the electrochemical corrosion behavior of polycrystalline diamond. *Carbon* **200**: 1–9 (2022)

[40] Schwarz U D. A generalized analytical model for the elastic deformation of an adhesive contact between a sphere and a flat surface. *J Colloid Interf Sci* **261**(1): 99–106 (2003)

[41] Hsia F C, Elam F M, Bonn D, Weber B, Franklin S E. Wear particle dynamics drive the difference between repeated and non-repeated reciprocated sliding. *Tribol Int* **142**: 105983 (2020)

[42] Hsia F C, Franklin S, Audebert P, Brouwer A M, Bonn D, Weber B. Rougher is more slippery: How adhesive friction decreases with increasing surface roughness due to the suppression of capillary adhesion. *Phys Rev Res* **3**(4): 043204 (2021)

[43] Hsia F C, Hsu C C, Peng L, Elam F M, Xiao C, Franklin S, Bonn D, Weber B. Contribution of capillary adhesion to friction at macroscopic solid–solid interfaces. *Phys Rev Appl* **17**(3): 034034 (2022)

[44] Luo Y R. *Comprehensive Handbook of Chemical Bond Energies*. Boca Raton (USA): CRC Press, 2007.

[45] Felts J R, Oyer A J, Hernández S C, Whitener K E, Robinson J T, Walton S G, Sheehan P E. Direct mechanochemical cleavage of functional groups from graphene. *Nat Commun* **6**: 6467 (2015)

[46] Carpick R W, Salmeron M. Scratching the surface: Fundamental investigations of tribology with atomic force microscopy. *Chem Rev* **97**(4): 1163–1194 (1997)

[47] Chen L, Qian L M. Role of interfacial water in adhesion, friction, and wear—A critical review. *Friction* **9**(1): 1–28 (2021)

[48] Jensen D S, Kanyal S S, Madaan N, Vail M A, Dadson A E,

Engelhard M H, Linford M R. Silicon (100)/SiO_2 by XPS. *Surf Sci Spectra* **20**(1): 36–42 (2013)

[49] Xiao C, Chen C, Yao Y Y, Liu H S, Chen L, Qian L M, Kim S H. Nanoasperity adhesion of the silicon surface in humid air: The roles of surface chemistry and oxidized layer structures. *Langmuir* **36**(20): 5483–5491 (2020)

[50] Ma H R, Bennewitz R. Nanoscale friction and growth of surface oxides on a metallic glass under electrochemical polarization. *Tribol Int* **158**: 106925 (2021)

[51] Dziaduszewska M, Shimabukuro M, Seramak T, Zielinski A, Hanawa T. Effects of micro-arc oxidation process parameters on characteristics of calcium-phosphate containing oxide layers on the selective laser melted $Ti_{13}Zr_{13}Nb$ alloy. *Coatings* **10**(8): 745 (2020)

Steve FRANKLIN. He received his bachelor's degree in material science from Sheffield Hallam University, UK, and his Ph.D. degree in metallurgy from Loughborough University of Technology, UK. He moved to the Netherlands in 1986 and has more than 35 years of experience in industrial research and development, researching and applying tribology, and material science and engineering principles within the healthcare, medical, consumer electronics, and semiconductor manufacturing industries. From 2017 to 2023, he built up and led the Contact Dynamics group at Advanced Research Center for Nanolithography (ARCNL), the Netherlands, and is Visiting Professor in Tribology at the University of Sheffield, UK and at University of Amsterdam (UvA), the Netherlands.

Chen XIAO. He is currently a postdoctoral researcher in Advanced Research Center for Nanolithography (ARCNL), the Netherlands. He earned his Ph.D. degree in mechanical design and theory from Southwest Jiaotong University, China, in 2019. His research focused on nanotribology.